

ROMP and RCM catalysed by $(R_3P)_2Cl_2Ru=CHPh$ immobilised on a mesoporous support

Karen Melis^a, Dirk De Vos^b, Pierre Jacobs^b, Francis Verpoort^{a,*}

^a Department of Inorganic and Physical Chemistry, Ghent University, Krijgslaan 281 (S-3), 9000 Gent, Belgium

^b Center for Surface Chemistry and Catalysis, Katholieke Universiteit Leuven, Kardinaal Mercierlaan 92, 3001 Leuven, Belgium

Received 19 September 2000; received in revised form 7 November 2000; accepted 5 December 2000

Abstract

Heterogeneous hybrid catalysts with respect to the metathesis of olefins have been prepared by ligand exchange reaction between Ru-alkylidene complexes (Grubbs' type) and a phosphinated mesoporous matrix (P-MCM-41). The host/guest interaction is studied by FT-Raman, thermogravimetric analysis and N_2 adsorption. Catalytic tests in olefin metathesis reveal ROMP activity towards norbornene, even in aquatic environment, and a very high activity for the RCM of diallylamine and diethyldiallylmalonate. © 2001 Elsevier Science B.V. All rights reserved.

Keywords: Ru-alkylidene; MCM-41 materials; Heterogeneous catalysis; Ring opening metathesis polymerisation; Ring closing metathesis

1. Introduction

Olefin metathesis has its roots in polymer chemistry, but it remained a laboratory curiosity in organic synthesis for decades, simply because most of the early metathesis catalysts are more or less incompatible with polar functional groups [1–3]. Since, the development of well defined metal alkylidene complexes, the opportunities for employing olefin metathesis have grown exponentially. Of the various catalysts reported that induce olefin metathesis, Grubbs' ruthenium catalyst $((R_3P)_2Cl_2Ru=CHPh)$ has attracted interest due to its ease of handling and substrate applicability [4,5]. The well-balanced electronic and coordinative unsaturation of the Ru(II) centre accounts for the high performance and the excellent tolerance of these complexes toward an array of polar functional groups. Immobil-

isation of the Ru-carbene complexes on a thermally and mechanically stable inorganic backbone combines the advantages of homogeneous catalysis and the ease of separation of heterogeneous catalysts. The grafting of the Ru complex on polystyrene-divinylbenzene (PS-DVB) polymers has been reported earlier [6]. The activity of the PS-DVB supported ruthenium carbene olefin metathesis catalysts is retarded in comparison to the homogeneous analogue. This is due, in case of ROMP, to diffusion limitations, which lower the metathesis rate. The decrease in the metathesis rate is offset by the extended lifetime and re-use of the solid phase Ru-vinyl-carbene. In 2000, Beerens et al. reported the chemical attachment of Ru-alkylidene complexes on carbosilane dendrimers [7]. Both the zeroth (G0) and the first (G1) generation were functionalised with the Ru complexes by an olefin metathesis reaction. The polydispersity exposed by the catalyst-dendrimer moieties were much lower compared to the PDI-enhancement of the PS-DVB supported catalysts.

* Corresponding author. Tel.: +32-9-264-4436;
fax: +32-9-264-4983.
E-mail address: francis.verpoort@rug.ac.be (F. Verpoort).

In 1992, the preparation of MCM-41 denotes a ground breaking development in hybrid catalysis [8]. The creation of a uniform mesoporous skeleton delivers a new mean of immobilisation. The large pore size allows large organic and organometallic molecules to pass through the channels and provides optimal contact with the surface. In addition, the regular pore size of MCM-41 can provide shape selectivity not provided by classical inorganic supports. Homogeneous catalysts RhR_3Cl ($\text{R} = \text{Ph}, \text{C}_3\text{H}_5$) have been successfully immobilised on solid supports through anchoring ligands [e.g. $-(\text{CH}_2)_n\text{PPh}_2$] ($n = 1, 2$) which are chemically bonded to the surface of the support [9–11]. In this paper, we report the synthesis, characterisation and activity of hybrid ruthenium alkylidene catalysts.

2. Experimental

2.1. General

All experiments were performed under purified inert gas by Schlenck techniques. Commercial grade solvents were dried and deoxygenated for at least 24 h over appropriate drying agents under nitrogen atmosphere and freshly distilled prior to use.

XRD data were collected by a Siemens diffractometer 5000, X-ray source = $\text{Cu K}\alpha$. Thermogravimetric analysis were performed with a TA Instruments 2000-951.

^1H NMR spectra were recorded at 500 MHz and 25°C on a Bruker AM spectrometer. Infrared spectra were performed on a Mattson 5020. Raman spectra were recorded on a Bruker equinox55/FRA 106. All spectra were recorded with a laser power of 100 mW. The laser (Nd) had a wavelength of 1064 nm. Nitrogen adsorption isotherms were recorded on a Micromeritics Gemini 2360 Surface Area Analyser with Flow prep 060 Degasser. The samples were dried overnight at 423 K and then cooled to room temperature prior to adsorption. Extra care with the functionalised materials was necessary due to the possibility of aerial oxidation, therefore, transfer to the balance and out gassing of the system was fast. Nitrogen isotherms were recorded at 77 K. Specific surface areas were determined from the linear part of the BET plot ($P/P_0 = 0.05\text{--}0.3$). GC-analysis is performed using the follow-

ing conditions: column: $\text{SPB}^{\text{TM}}\text{-5}$; $30\text{ m} \times 0.25\text{ mm} \times 0.25\text{ }\mu\text{m}$ film thickness; carrier gas: He, 100 kPa; detector: FID; gas chromatograph: Varian 3300; integrator: Vista 401. GPC (THF) conditions: column, PL gel 5 μm mixed-C (60 cm, $d = 7.5\text{ mm}$); detector, refraction index (RI) Knauer differential diffractometer and flow = 1 ml min^{-1} (concentration: 2%).

2.1.1. $(\text{EtO})_3\text{Si}(\text{CH}_2)_x\text{PR}_2$ ($\text{R} = \text{Ph}, \text{Cy}$) and $x = 2\text{--}3$

To a solution of $(\text{EtO})_3\text{Si}(\text{CH}_2)_x\text{Cl}$ in diethylether-1 equivalent of BuLi is added dropwise at -78°C . Next one equivalent PR_2Cl is added and the formed LiCl is filtered off. The solvent is removed in vacuo.

$(\text{EtO})_3\text{Si}(\text{CH}_2)_2\text{PPh}_2$: ^1H NMR (500 MHz, 25°C, CDCl_3): 7.75 (t, 4H, *m*-H C_6H_5), 7.52 (t, 2H, *p*-H C_6H_5), 7.35 (d, 4H, *o*-H C_6H_5), 3.70 (q, 6H, $\text{CH}_3\text{--CH}_2\text{--O}$), 2.10 (t, 2H, $\text{CH}_2\text{--P}$), 1.02 (t, 9H, $\text{CH}_3\text{--CH}_2\text{--O}$), 0.72 (q, 2H, $\text{CH}_2\text{--Si}$). IR (KBr, cm^{-1}) 3070, 3054, 2950, 2850, 1600–2000, 1470, 1435, 1050–1200. FT-Raman (cm^{-1}) 3055, 2990, 2890, 1588, 1000.

$(\text{EtO})_3\text{Si}(\text{CH}_2)_3\text{PCy}_2$: ^1H NMR (500 MHz, 25°C, CDCl_3): 0.65 (t, 2H, Si--CH_2), 1.2–1.7 (m, 31H, *P*-Cy and $\text{CH}_3\text{--CH}_2\text{--O--Si}$), 1.8–2.1 (m, 4H, $\text{Si--CH}_2\text{--}(\text{CH}_2)_2\text{--P}$), 3.8 (m, 6H, $\text{CH}_3\text{--CH}_2\text{--O}$). IR (KBr, cm^{-1}) 2936, 2852, 1445, 1030, 818. FT-Raman (cm^{-1}) 2936, 2852, 1445, 1030, 818.

2.1.2. MCM-41

MCM-41 was synthesised as described previously [12]. After calcination the mesoporous material was characterised by XRD, N_2 adsorption and Raman spectroscopy. MCM-41 is dried overnight in vacuo at 130°C to achieve complete thermodesorption of physically adsorbed water molecules from the silica surface.

2.1.3. Phosphinated MCM-41 (*P*-MCM-41)

In a typical experiment 1 g MCM-41 is suspended in 10 ml toluene. 1.5 mmol of the phosphine spacermolecule is added. The reaction mixture is stirred at reflux temperature overnight. The modified MCM-41 is allowed to settle down at room temperature. The excess of spacermolecule was removed by a lengthy soxhlet extraction using a diethylether–dichloromethane mixture (1/1). The loading of the $(\text{EtO})_3\text{Si}(\text{CH}_2)_2\text{PPh}_2$ modified MCM-41 amounts to 9.4 wt.% and the

(EtO)₃Si(CH₂)₃PCy₂ modified MCM-41 amounts to 12 wt.% phosphine.

2.1.4. Anchoring of (R₃P)₂Cl₂Ru=CHPh on phosphinated MCM-41

To 1 g of dried P-MCM-41 a solution of 1.5 mmol of (R₃P)₂Cl₂Ru=CHPh in dichloromethane is added. The reaction mixture is stirred overnight at room temperature. The solid is filtered, washed with toluene and dichloromethane and dried in vacuo. Loadings of 0.76 wt.% Ru per gram MCM-41 for complex (Ph₃P)₂Cl₂Ru=CHPh and 0.96 wt.% Ru per gram MCM-41 for complex (Cy₃P)₂Cl₂Ru=CHPh are established by thermogravimetric analysis. The TGA spectra reveal a thermal stability of 200°C for the anchored (Ph₃P)₂Cl₂Ru=CHPh complex and 212°C for the supported (Cy₃P)₂Cl₂Ru=CHPh complex.

2.1.5. ROMP of norbornene

To 0.005 mmol catalyst is added 150 equivalent of a norbornene solution (RT, CH₂Cl₂). To stop the polymerisation reaction, 2–3 ml of an ethylvinylether/BHT solution is added and the solution is stirred till the deactivation of the active species is completed. The solution is poured into 50 ml methanol (containing 0.1% BHT) and the polymers are precipitated and dried in vacuum overnight.

2.1.6. ROMP of norbornene in H₂O

Boiling distilled water is deoxygenated by bubbling N₂. To 0.06 mmol catalyst, suspended in 7 ml H₂O, 150 equivalents of norbornene are added. The reaction is stirred at 70°C for 15 h. After dissolving the polymer in CHCl₃ and separation of catalyst and polymer by filtration, the same procedure as for ROMP of norbornene in organic media is followed for the isolation of the polymers.

2.1.7. Ring closing metathesis

A solution of 0.5 mol% catalyst, substrate and internal standard are stirred for, respectively, 0.5, 1 and 2 h at room temperature in CH₂Cl₂ or CCl₄ and at 60°C in CCl₄. The two substrates examined are diethyldiallylmalonate (internal standard = dodecane) and diallylamine (internal standard = *n*-octane). The ring closing metathesis reaction is monitored by GC. The formation of the reaction products is confirmed using ¹H NMR.

3. Results and discussion

3.1. Synthesis

The grafting of the Grubbs' catalyst on the mesoporous material was performed in two steps. First the silica surface was functionalised with a phosphine spacer molecule which anchored the homogeneous catalyst in the second step by ligand exchange (Schemes 1 and 2).

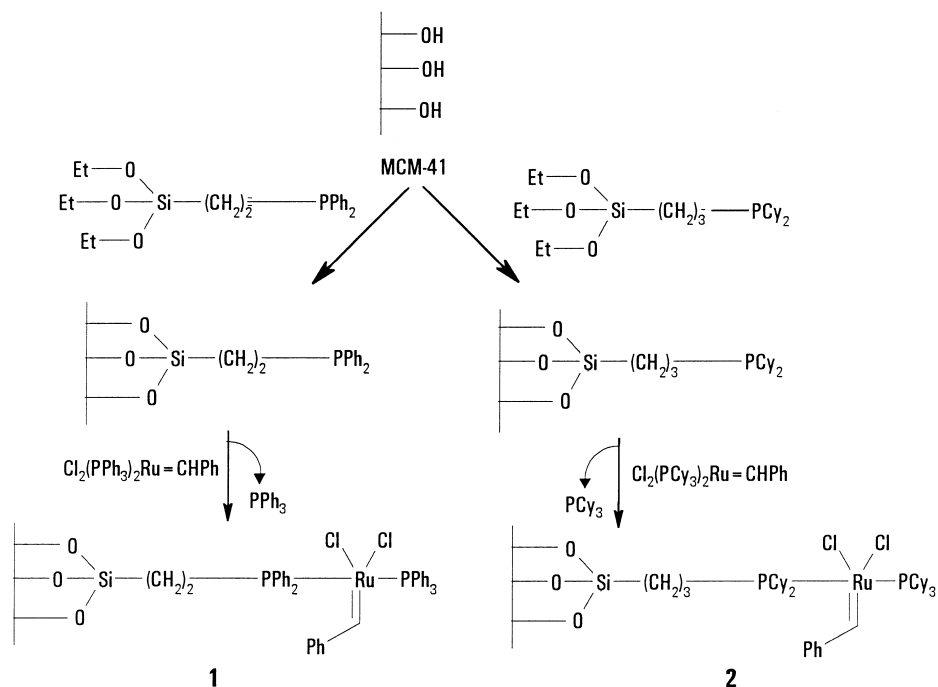
The exchange of a PR₃ ligand of the homogeneous complex by the PR₂ functionality of the spacer molecule was favoured due to the increasing p*K*_a or donor capacity of the phosphine. The (Ph₃P)₂Cl₂Ru=CHPh homogeneous catalyst (**1**) was attached to the siliceous surface using diphenylphosphinoethyltriethoxysilane (DIPPS) as linkermolecule. The (Cy₃P)₂Cl₂Ru=CHPh complex (**2**) is anchored using dicyclohexylphosphinopropyltriethoxysilane (DICPS) to modify the support. Again ligand exchange is preferred due to an increase in donor capacity. Since the p*K*_a of the linkermolecules are unknown, an alternative deduction of the donor capacity was performed. Various phosphines with an established p*K*_a are modelled by a semi-empirical molecular orbital method [13]. The calculated electronic densities of the, respectively, P-atoms are plotted versus the established p*K*_a values (Fig. 1).

The two linkermolecules are also modelled using the same semi-empirical method. The electronic densities on the, respectively, P-atoms are calculated and the p*K*_a is deducted from the p*K*_a versus electronic density plot. The p*K*_a of DIPPS amounts to 3.15 which exceeds the p*K*_a of the PPh₃ ligand of the Ru-complex (=2.72). The same result was obtained for the PCy₂ linkermolecule (10.30) versus the PCy₃ ligand (9.89).

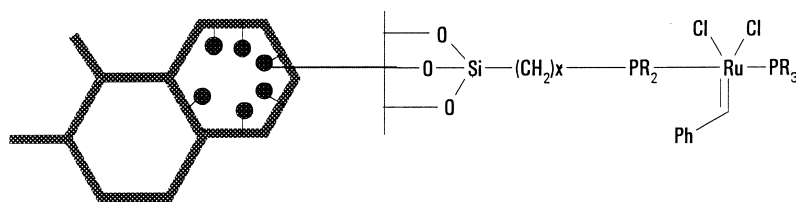
3.2. Characterisation

3.2.1. X-ray diffraction

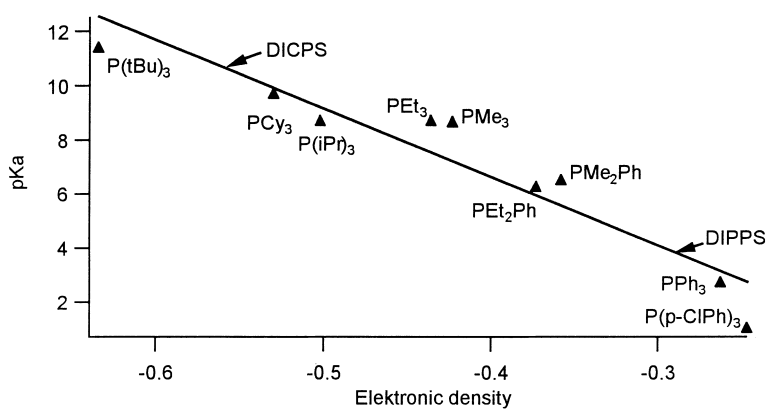
Powder X-ray diffraction data for calcined MCM-41 is shown in Fig. 2. The observation of three peaks is indexed as a hexagonal lattice which is typical of MCM-41 materials. The hexagonal lattice parameter, *a*₀ (= 2*d*₁₀₀/√3), is 44.45. The wall thickness, calculated by subtracting the channel diameter (*D*_{BJH} = 2.7 nm) from the unit cell parameter (*a*₀) is 1.7 nm.



Scheme 1. Reaction sequence of the immobilisation of Grubbs' type metathesis catalysts.



Scheme 2. Schematic illustration of anchored Ru catalyst in MCM-41.

Fig. 1. pK_a vs. electronic density (modelled by semi-empirical molecular orbital method: Parameterization Method 3 (PM3), Spartan Version 1997).

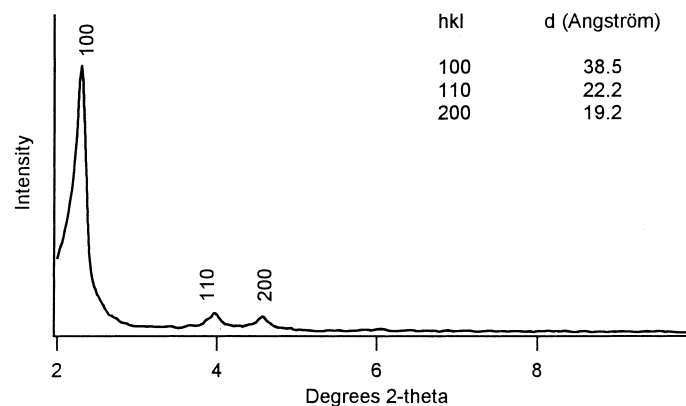


Fig. 2. X-ray diffraction of pristine MCM-41.

3.2.2. Raman spectroscopy

The anchoring of the Grubbs' catalyst on the mesoporous catalyst was checked using Raman spectroscopy (Fig. 3). The low intensity scattered by the mesoporous support makes it possible to examine the grafting of, respectively, the linkermolecule and the homogeneous catalyst. The comparison of the Raman spectra of P-MCM-41 and the molecular sieve clearly indicates the grafting of the spacermolecule. The superposition of the signals originating from the spacermolecule is clearly shown. An indication for ligand exchange, from the comparative study of P-MCM-41 and the supported $(\text{Ph}_3\text{P})_2\text{Cl}_2\text{Ru}=\text{CHPh}$ catalyst (**1**), is the wavenumber shift from 1593 to 1608 cm^{-1} (Ph ring stretch) and the signal characteristic for the CH-stretch of the benzylidene is marked at 3016 cm^{-1} . Thus, the comparison of the Raman spectrum of the homoge-

neous and hybrid catalyst is performed to eliminate any doubt concerning the chemical attachment of the Grubbs' catalyst (Table 1).

The wavenumber shift from 1592 to 1608 cm^{-1} indicates a change in the aromatic environment and the shift from 288 to 274 cm^{-1} reveals a different chemical environment for the P–C bond. The anchoring of the homogeneous complex $(\text{Cy}_3\text{P})_2\text{Cl}_2\text{Ru}=\text{CHPh}$ on P-MCM-41 (**2**) reveals the same wave shifts as for **1**. Comparison of the free complex and the anchored equivalent reveals wavenumber shifts at 1456–1448 cm^{-1} (CH_2 -scissors), 1253–1297 cm^{-1} (CH_2 in-plane twist), 802–821 cm^{-1} (ring breathing of Cy) and 227–223 cm^{-1} (P–C vibration), which clearly indicates the chemical attachment of the homogeneous $(\text{Cy}_3\text{P})_2\text{Cl}_2\text{Ru}=\text{CHPh}$ catalyst on the modified silica surface.

Table 1
Raman analysis of free and anchored complex of **1** and **2**

Complex	Vibration	Free complex (cm^{-1})	Anchored complex (cm^{-1})
1	Aromatic CH stretch	3059	3063
	Ring stretch	1588	1608
	In-plane CH deform	1031	1029
	P–C vibration	288	274
2	CH_2 scissors Cy	1456	1448
	CH_2 in-plane twist	1253	1297
	Ring breathing Cy	802	821
	P–C vibration	227	223

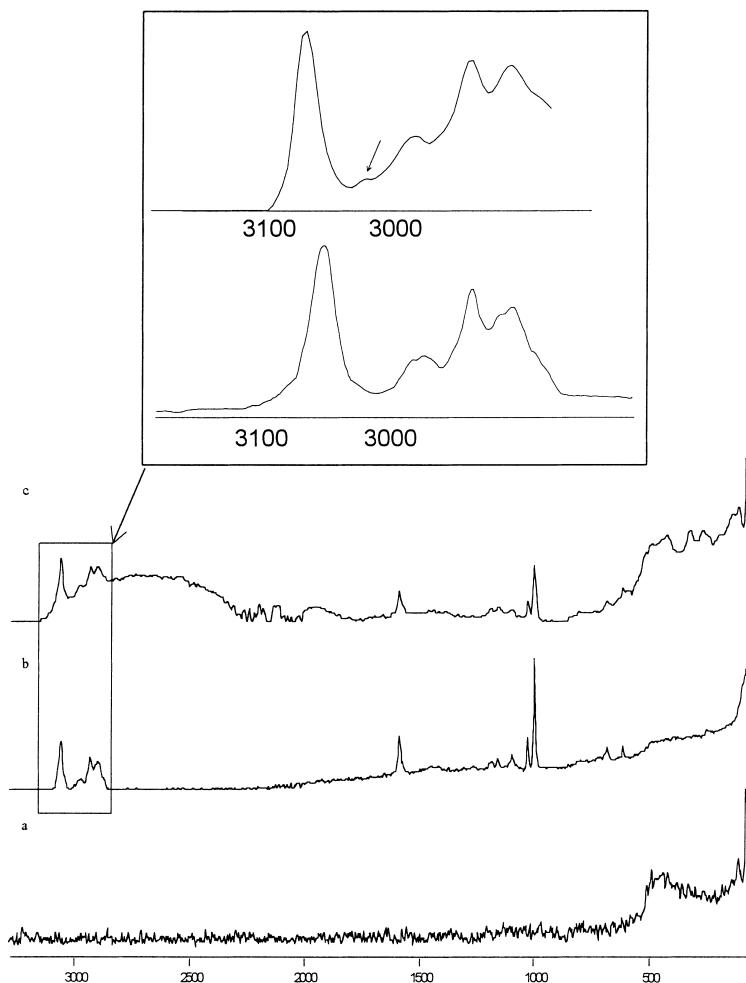


Fig. 3. Raman analysis of anchoring of $(\text{Ph}_3\text{P})_2\text{Cl}_2\text{Ru}=\text{CHPh}$ on mesoporous support: (a) pristine MCM-41; (b) P-MCM-41; (c) **1**.

3.2.3. N_2 adsorption analysis

The N_2 adsorption–desorption isotherms of the pristine MCM-41 at 77 K is similar to that reported previously for MCM-41-type mesoporous solids (Fig. 4a). It is defined as a reversible Type IV IUPAC classification, and until now has only been encountered for MCM-41 materials [14–16]. At low relative pressure ($P/P_0 = 0.3$) the adsorbed volume increases linearly with increasing pressure. This region corresponds to a monolayer–multilayer adsorption on the pore walls. Between $P/P_0 = 0.3$ and 0.4 there is a sharp increase in the adsorbed volume, attributed to the capillary condensation. At higher relative pressure multilayer ad-

sorption takes place on the external surface, resulting in a gradual increase of the adsorbed volume. At $P/P_0 = 1$ a saturation was reached which indicates that all mesopores are filled with the condensed adsorbens. The BET surface area was calculated to be $1484 \text{ m}^2 \text{ g}^{-1}$ and the adsorption porevolume amounts to $1.04 \text{ cm}^3 \text{ g}^{-1}$.

Reversible Type IV IUPAC isotherms similar to the pristine MCM-41 were obtained for P-MCM-41 and the anchored catalyst, respectively, providing strong evidence that the mesoporous structure of the silica support was retained throughout the grafting process and that the channels remained accessible (Fig. 4b–c).

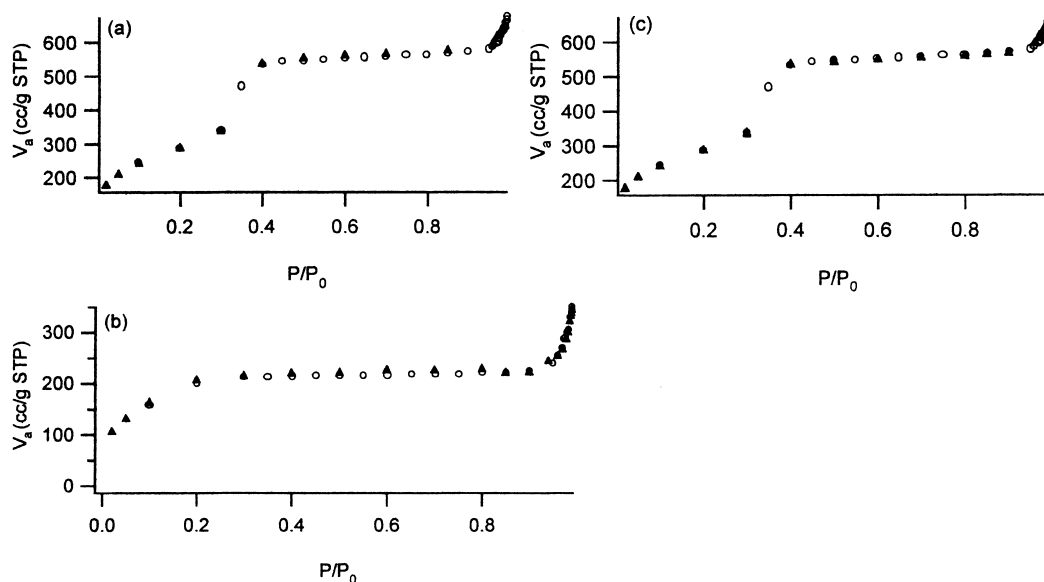


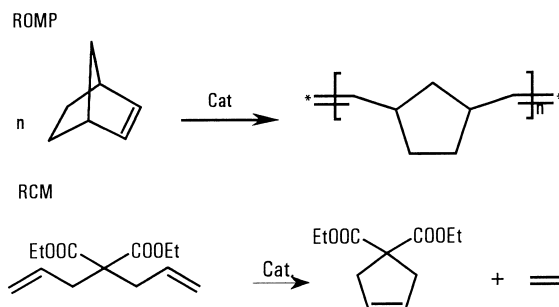
Fig. 4. N_2 adsorption-desorption isotherms recorded at 77 k of MCM-41 samples: (a) pristine MCM-41; (b) P-MCM-41; **1**. Circles denote adsorption, triangles denote desorption.

The BET surfaces were calculated for both catalysts as 738 and 752 $m^2 g^{-1}$ for **1** and **2**, respectively (Table 2).

This approximate 50% decrease can be attributed to the successfully anchoring of the Grubbs' catalyst on the internal surfaces of the mesoporous material. This is confirmed by the decrease of the adsorption pore volume to 0.63 and 0.65 $cm^3 g^{-1}$, respectively.

3.3. Catalysis

The catalytic activity of both heterogeneous complexes was investigated for both ring opening metathesis polymerisation (ROMP) and ring closing



Scheme 3. ROMP of norbornene and RCM of diethyldiallylmalonate.

metathesis (RCM). In Scheme 3, both reactions are schematically depicted.

3.3.1. Ring opening metathesis polymerisation (ROMP)

The ROMP of norbornene catalysed by **1** is the first test reaction performed (Fig. 5). At room temperature the conversion reaches, after a 90 min increase, a stable value of 70% and remains steady.

The ROMP yields elastomers where the double bond, which has a variable stereochemistry, is

Table 2
 N_2 -adsorption analysis of successive grafting process of catalyst **1** and **2**

Catalyst	Stage	Specific surface ($m^2 g^{-1}$)	Pore volume ($cm^3 g^{-1}$)
1	MCM-41	1484	1.04
	P-MCM-41	799	0.74
	Catalyst	738	0.63
2	MCM-41	1484	1.04
	P-MCM-41	810	0.70
	Catalyst	752	0.65

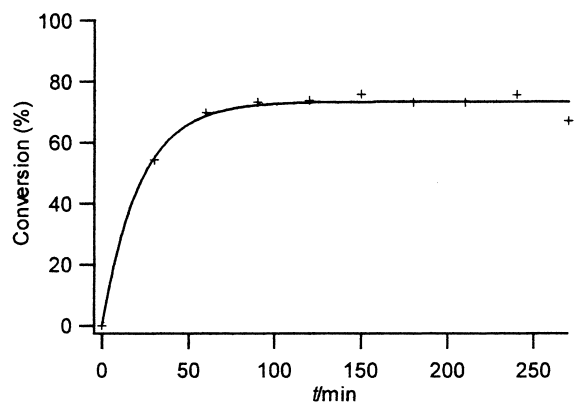


Fig. 5. ROMP of norbornene catalysed by **1**. Reaction conditions: room temperature, catalyst/monomer: 1/150, CH_2Cl_2 .

retained in the product. This stereochemistry of the double bond was determined by ^1H NMR and a *cis/trans* ratio of 16/84 was calculated. The polydispersity index (PDI) tends to be much higher than normally achieved with the homogeneous analogue. The ROMP of norbornene catalysed by the homogeneous $\text{Cl}_2(\text{PR}_3)_2\text{Ru}=\text{CHPh}$ complex yields a polymer with a PDI (toluene) ranging from 1.04 to 1.10 in contrary to the PDI (THF) obtained with the hybrid catalyst (Table 3) [17].

In contrast to the different catalytic species, obtained by Grubbs et al., by grafting the Ru-carbene on a phosphine functionalised PS-DVB resin, the two different catalytic species possibly formed here, are the coordination of one or two neighbouring spacermolecules. Calculations show a PR_2 -spacer occupation onto the mesoporous material of one spacer per 44 nm^2 . The loading was calculated from the TGA weight loss and the specific surface from N_2 measurements. Thus, the opportunity to form a

two-spacermolecule Ru-complex species is statistically neglectable.

The same test reaction was performed catalysed by **2**, but gelation occurred immediately, so it was impossible to retrieve a conversion versus time plot. This phenomenon results in a high polydispersity caused by diffusion limitations and back-biting reactions. In contrast to the homogeneous catalyst where both the catalyst and the olefin are dispersed throughout the solution, the heterogeneous olefin metathesis reaction is limited by the diffusion of the olefins into the channels of MCM-41. The presence of the polymer in the channels can block the transport of residual monomer into the pores and thus, to the active sites. Since the $\text{Ru}=\text{C}$ is dispersed in the channels backbiting can occur, not only by the same catalytic centre, but even by the neighbouring active sites. The high PDI values are solely caused by diffusion and backbiting due to the appearance of only one kind of active site. The results obtained for the homogeneous complex are similar.

The ROMP of norbornene was also performed in deoxygenated water. The conversion reached 55% after 15 h. This means that the heterogeneous catalyst is capable to exhibit ROMP activity in aquatic environment. The elevated PDI (4.75 (THF)) is due to the influence of the media. The ability to exhibit ROMP activity in aquatic media is contradictory to data obtained for the homogeneous equivalent. This can be explained by the ease of suspending the catalyst in its heterogeneous state, whereas in the homogeneous form the insolubility impedes the creation of a homogeneous reaction environment.

3.3.2. Ring closing metathesis (RCM)

Since, in the last decade scientific research on the possibility of RCM has grown exponentially. It has shown to be an excellent tool in the synthesis of challenging pharmaceutical and natural products.

Table 3
ROMP of norbornene using the hybrid catalysts

Catalyst	Temperature ($^{\circ}\text{C}$)	Solvent	M_n	M_w	<i>cis/trans</i> (%) ^a	PDI ^b
1	RT	CH_2Cl_2	8.340	60.000	16/84	7.2
2	60	Cl-Ph	18.000	49.000	20/80	2.72
	70	H_2O	31.032	147.498	15/85	4.75

^a Determined with ^1H NMR (500 MHz, 25°C , CDCl_3).

^b PDI (THF).

Table 4
Percent conversions of 5 mol% catalysts **1–3** for RCM

Run	Catalyst	Substrate ^a	Temperature (°C)	Solvent	Time (h)	Conversion (%)
1	1	A	35	CH ₂ Cl ₂	1	11
2			60	CCl ₄	1	51
3		B	35	CH ₂ Cl ₂	1	34
4			60	CCl ₄	1	100
5	2	A	RT	CH ₂ Cl ₂	0.5	71
6			60	CCl ₄	2	57
7		B	RT	CH ₂ Cl ₂	0.5	100
8			60	CCl ₄	0.5	100
9	3	A	RT	CCl ₄	0.5	98
10			60	CCl ₄	0.5	86
11		B	RT	CCl ₄	0.5	100
12			60	CCl ₄	0.5	100

^a A: diethyldiallylmalonate; B: diallylamine.

Controlled stereochemistry was obtained using the Grubbs' catalyst and derivatives. These exciting revelations tempted us to study the ring closing metathesis activity of the heterogeneous hybrid catalysts. The RCM activity was tested using diethyldiallylmalonate and diallylamine as test substrates and was followed by GC-analysis (Table 4).

Of the heterogeneous systems, **2** exhibits the highest activity (runs 1–4 versus runs 5–8). This is due to the ligand effect of the phosphine moiety. Grubbs et al. [18] proved that larger and more electron donating phosphines produce more active catalysts. The RCM activity of the homogeneous (Cy₃P)₂Cl₂Ru=CHPh complex (**3**) is slightly higher compared to the activity depicted for the heterogeneous equivalent **2** (runs 5–8 versus runs 9–12). The decrease for the RCM of diethyldiallylmalonate is clearly influenced by diffusion limitations due to the use of a carrier.

Another striking difference is the decrease in conversion for the RCM of diethyldiallylmalonate from room temperature to 60°C for both the homogeneous and the heterogeneous (Cy₃P)₂Cl₂Ru=CHPh catalyst (respectively, runs 5–6 and 9–10). This phenomenon is not shown for the conversion of diallylamine. The reason is the higher affinity of the catalytic species for diallylamine. The ring closing metathesis of diallylamine proceeds at a higher rate compared to the metathesis of diethyldiallylmalonate, where thermal deactivation of the catalyst influences the amount of converted diene. Thermal deactivation occurs during

the metathesis reaction which lowers the conversion rates.

Minor leaching was observed after ring closing metathesis reaction. Quantitative Ru residu analysis of the filtrate was obtained by ICP-MS analysis. The contaminant level was just 3.2% for catalyst **1** and 1.2% for catalyst **2** of the Ru in the original catalyst. Calculations show that 25% of the spacermolecules coordinate a Ru-carbene. The results were obtained from a combination of TGA and BET data of both P-MCM-41 and both catalysts (**1** and **2**). In analogy to the "boomerang" catalyst, recapture of a fraction of the leached Ru-complex occurs. A fraction of the catalyst becomes homogeneous for the course of the metathesis reaction and is then recaptured by the uncoordinated phosphine spacermolecules after completion of the solution reaction [19].

4. Conclusions

Immobilisation of Grubbs' type catalysts on phosphinated inorganic mesoporous silicas was carried out. N₂ adsorption studies confirm that the textural properties are retained throughout the grafting process. The condensation reaction between the surface and the spacermolecule and the ligand exchange reaction between the phosphinated support and the homogeneous catalysts were confirmed with Raman spectroscopy and thermogravimetric analysis.

Due to diffusion limitations an enhancement in polydispersity was exhibited for the ROMP of norbornene catalysed by **1**. Catalyst **2** even exposes metathesis activity in aquatic environment.

The RCM activity is in good agreement with the activity of the homogeneous catalysts. Literature data of the homogeneous analogue of **2** proved to be ring closing a broad variety of di-olefins. In this perspective catalyst **2**, the heterogeneous equivalent of the Grubbs catalyst, holds great promise for the synthesis of fine chemicals.

Acknowledgements

K.M. is indebted to the BOF (Bijzonder Onderzoeksfonds) of Ghent University for a research grand. We are indebted to FWO (Fonds voor Wetenschappelijk Onderzoek-Vlaanderen) for a research grand (D.D.V., P.J., F.V.). Thermogravimetric analysis of the LUC-Diepenbeek (Professor J. Mullens, Professor L. Van Poucke and S. Mullens) was greatly acknowledged.

References

- [1] M. Randall, M. Snapper, *J. Mol. Catal. A: Chem.* 133 (1998) 29.
- [2] K. Ivin, *J. Mol. Catal. A: Chem.* 133 (1998) 1.
- [3] M. Schuster, S. Blechert, *Angew. Chem. Int. Ed. Engl.* 36 (1997) 2036.
- [4] S. Nguyen, R. Grubbs, *J. Am. Chem. Soc.* 115 (1993) 9858.
- [5] P. Schwab, M. France, J. Ziller, R. Grubbs, *Angew. Chem. Int. Ed. Engl.* 34 (1995) 2039.
- [6] S. Nguyen, R. Grubbs, *J. Organomet. Chem.* 497 (1995) 195.
- [7] H. Beerens, F. Verpoort, L. Verdonck, *J. Mol. Catal. A: Chem.* 151 (2000) 279.
- [8] J. Beck, J. Vartuli, W. Roth, M. Leonowicz, C. Kresge, K. Schmitt, C. Chu, D. Olson, E. Sheppard, S. McCullen, J. Higgins, J. Schlenker, *J. Am. Chem. Soc.* 114 (1992) 10834.
- [9] R.H. Grubbs, L.C. Kroll, *J. Am. Chem. Soc.* 93 (1971) 3062.
- [10] K.G. Allum, R.D. Hancock, I.V. Howell, T.E. Lester, S. McKenzie, R.C. Pitketly, P.J. Robinson, *J. Catal.* 43 (1976) 331.
- [11] S. Shyu, S. Cheng, D. Tzou, *Chem. Commun.* 21 (1999) 2337.
- [12] I. Vankelecom, N. Moens, K. Vercruyse, R. Parton, P. Jacobs, *Studies in Surface Science and Catalysis: Heterogeneous Catalysis and Fine Chemicals IV*, H.U. Blaser, A. Baiker, R. Prins, Elsevier Amsterdam, 1997, p. 724.
- [13] Molecular Modelling was performed using PM3 methods (J. Stewart, *J. Comput. Chem.*, 10 (1989) 209 and J. Stewart, *J. Comput. Chem.*, 10 (1989) 221) as implemented in SPARTAN (PC Spartan Plus, Wavefunction Inc., 18401 Van Karman Ave., Ste. 370, Irvine, CA 92612 U.S.A.).
- [14] O. Franke, G. Schulz-Ekloff, J. Rathousky, J. Stárek, A. Zúkal *Chem. Commun.* (1993) 724.
- [15] U. Ciesla, F. Schüth, *Microporous Mesoporous Mater.* 27 (1999) 131.
- [16] P. Branton, P. Hall, K. Sing, *Chem. Commun.* 16 (1993) 1257.
- [17] P. Schwab, R. Grubbs, J. Ziller, *J. Am. Chem. Soc.* 118 (1996) 100.
- [18] E. Dias, S. Nguyen, R. Grubbs, *J. Am. Chem. Soc.* 119 (1997) 3887.
- [19] M. Ahmed, A. Barrett, P. Braddock, S. Cramp, P. Procopiou *Tetrahedron Lett.* (1999) 8657.